

Simple crowd dynamics to generate complex temporal contact networks

Razieh Masoumi^{1,2}, Juliette Gambaudo¹, and Mathieu Génois^{1*}

¹ Aix-Marseille Université, CNRS, CPT, Marseille, France and

² Department of Molecular Medicine, University of Padova, Italy.

(Dated: May 13, 2024)

Empirical contact networks or interaction networks demonstrate peculiar characteristics stemming from the fundamental social, psychological, physical mechanisms governing human interactions. Although these mechanisms are complex, we test whether we are able to reproduce some dynamical properties of these empirical networks from relatively simple models. In this study, we perform simulations for a range of 2D models of particle dynamics, namely the Random Walk, Active Brownian Particles, and Vicsek models, to generate artificial contact networks. We investigate temporal properties of these contact networks: the distributions of contact durations, inter-contact durations and number of contact per pair of particle. We demonstrate that the distribution of inter-contact durations can be recovered by the dynamics of these simple crowd particle models, and show that it is simply related to the well-know first-return process, which explains the $-3/2$ exponent that is found in both the numerical models and empirical contact networks.

INTRODUCTION

Temporal networks, characterized by dynamic interactions and evolving connections over time, have gained significant attention across various disciplines in recent years, precisely because of their evolving nature. These networks capture essential aspects of real-world systems, where relationships, interactions, and information flows are highly time-dependent. Analyzing temporal networks provides valuable insights into numerous fields, including ecology [1, 5, 9, 46, 47] disease spreading [22, 29, 51], transportation [35], neuroscience [3, 4, 30], communication networks such as mobile phone calls [21, 25, 32] and email networks [11, 12], as well as citation networks [41, 42].

The structures and properties of temporal networks constrain processes which unfold on top of them. While understanding the effect of these structures is usually done with randomisation techniques [14, 16, 18, 19], generative models are needed to understand their origin. In the realm of generative models for temporal networks, there exist several noteworthy approaches, including but not limited to the following approaches. Holme introduced a fundamental technique known as “Static networks with link dynamics” [17, 39]. In this approach a temporal network is created by firstly generating a static network using a specific model and then generating a sequence of contacts for each link, typically without considering the network position of the links. Perra et al. [37] introduced an even more simplified model of temporal networks using a graph sequence framework. The approach involves increasing a time counter to t and initializing an empty simple graph G_t . For each node i , activation occurs with a probability $a_i \Delta t$, connecting i to m other randomly selected nodes, whether active or not. The probability a_i follows a truncated power-law distribution. The networks constructed in this way are

called Activity-driven networks [28]. Other approaches tried to take into account the intrinsic heterogeneous properties of the dynamics of empirical networks by implementing reinforcement processes, such as link-node memory models [49], and Self-exciting point processes [7, 31].

Among temporal networks, proximity networks, which describe how individuals interact with each other in the physical space, are of particular interest for various contexts such as disease transmission, information dissemination, crowd management during disasters, and more. In this regard, the study of temporal networks from a socio-temporal perspective has acquired significant attention in recent years, primarily linked to the emergence of contemporary data collection techniques such as GPS [8], and RFID chips [2, 23, 36, 50]. With the aid of advanced technology and data collection techniques, researchers can now analyze these networks in great detail, shedding light on the dynamics and patterns that govern our social exchanges. In this context, a groundbreaking investigation was the Reality Mining project, which involved outfitting Massachusetts Institute of Technology students with cell phones. These phones were equipped with Bluetooth technology capable of sensing their closeness to fellow individuals [10]. Another relevant effort in this area is the SocioPatterns Project, which has devised a mechanism for gauging physical closeness through wearable badges incorporating radiofrequency identification devices (RFID) [6]. Within this initiative, they have successfully constructed closed gathering temporal networks for various groups, including hospital patients [20], conferences participants [45], and students in schools [13].

As these networks arise from interactions between agents in the physical space, they may be intrinsically different from other classes of temporal networks which emerge from non spatial interactions (such as communication networks for example). Among generative mod-

els for temporal networks, few have tried to tackle the class of face-to-face interaction networks specifically, and thus a comprehensive theoretical understanding of face-to-face interaction data remains elusive. However, the underlying spatial aspect of their origin allows to take a different approach in their generative process. Starnini’s research, which introduces a dynamic framework for human interactions, is a pioneering work in this field [44]. The framework utilizes a two-dimensional random walk, with each agent possessing an attractiveness factor that influences the pace of movement for individuals in their proximity. This approach provides valuable insights into the dynamics of human interactions. However, the relation between spatial constraints and the properties of the temporal network of interactions remain unclear.

Previous analysis of empirical contact networks, and in particular the SocioPatterns datasets, have shown that specific dynamic features such as contact duration and inter-contact duration distributions exhibit similar properties across various contexts [44]. While acknowledging the inherent complexities of these networks, a compelling question arises: Can we capture some of their dynamic characteristics using simpler contact models? In this regard, we explore the feasibility of understanding empirical contact networks through the lens of relatively simple contact models which take into account the spatial origin of the contacts. Specifically, we focus on 2D particle dynamics, and we investigate the behavior of three distinct models: the Random Walk, the Active Brownian Particle model, and the Vicsek model. The first one is the simplest model for the dynamics of particles; the second one allows to introduce some limited memory effect on the trajectory, and the third one is one of the simplest models for motion of active matter exhibiting collective behavior.

Our primary objective is to generate contact networks from each of these 2D particle models and analyze the temporal aspects of these networks. We focus on three distributions: contact duration, inter-contact duration, and the number of contacts per pair of particles. By scrutinizing these temporal patterns, we aim to discern which aspects of empirical contact networks can be elucidated through the dynamics of these straightforward crowd particle models and which aspects necessitate additional mechanisms or complexities to achieve accurate representation.

One key finding of our investigation is the consistent presence of heavy-tailed distributions in the inter-contact duration, irrespective of the specific particle model employed. This interesting observation suggests that, though sociological, psychological, neurological and biological mechanisms are at play in human interactions, some patterns can be explained by a very simple, purely statistical effect. Indeed, we manage to connect the shape of the distribution of inter-contact durations to a simple first-return time problem, and recover the empirical ex-

ponent of -1.5 observed in all models and datasets.

METHODS

Models

Our primary objective is to understand the properties of empirical contact networks by exploring what happens for basic interaction models. One question in particular we aim to address is whether there exist universal properties that remain independent while varying the contact dynamics. To achieve this, we use three distinctive two-dimensional particle dynamics models: Random Walk, Active Brownian Particle, and Vicsek model. Fig. 1 shows a schematic explanation for the dynamics of a single particle between two consecutive time steps in each model. In all models we first assume that the particles are point-wise entities, which means their presence does not influence each other; their trajectories remain unchanged when they meet. In a second version, particles have a fixed size, and simply stop at contact.

We consider in all cases a system containing $N = 1000$ point-wise particles confined within a $2D$ box of side length $L = 100$. We have chosen this particular density for the particles to ensure comparability with the density of people in the conference data sets we have utilized [14]. After setting random initial conditions, the particles are observed to move freely within the box. When they encounter the boundaries, they undergo classic reflection due to the reflective boundary conditions. For completeness, we further tested the models with periodic boundary conditions or on an infinite space.

We deliberately adopt these relatively simple particle models and make their contact network, aiming to uncover potentially reproducible properties of empirical contact networks, even within the context of basic pedestrian models. While these models are widely explored, we aim to provide a concise yet comprehensive explanation of each of them, providing a clear understanding of their characteristics and relevance to our study.

Random walk

In the 2D Random Walk, each walker selects a random direction at each subsequent step, uniformly distributed between 0 and 2π , with a step length of Δr . The value of Δr is drawn at random in the positive half of a Gaussian distribution of mean 0 and of variance $D*dt$, where D and dt represent the diffusion coefficient and time increment at each step respectively. This continuous randomness in the particle’s movements is classically known to be a good model for a brownian motion [27]. The diffusion coefficient allows us to control the characteristics of the random walk. For a given time increment dt , a larger

diffusion coefficient implies that the random walker is more likely to move and spread rapidly throughout its surrounding space.

Active Brownian Particles (ABP)

The Active Brownian Particle (ABP) model adds a layer of complexity by adding a memory aspect into the particle motion. In the classical version of this model, particles undergo both a Brownian motion and a deliberate movement (usually the consequence of internal energy sources or external driving forces). In our simplified version, we exclude Brownian motion affecting position and focus solely on the self-propulsion of particles [40].

In practice, particles are constrained at each time step to select a new orientation uniformly within a specific range of angles, namely $\Delta\theta = [-\frac{\theta}{2}, \frac{\theta}{2}]$ around their current orientation, while maintaining a constant velocity v .

In this model, trajectories of particles exhibit a persistence of the angle over the persistence length, which increases as the angle range $\Delta\theta$ decreases. Note that for $\Delta\theta = 2\pi$, the ABP model is simply the 2D Random Walk with fixed step length.

Vicsek model

The Vicsek model focuses on collective behavior emerging from local interactions among self-propelled particles. Inspired by the movement of flocks of birds or schools of fish, this model assumes that particles align their velocities with those of their neighbors within a certain interaction radius R_n , while accounting for uncertainties caused by noise η_i . This alignment is mathematically described by the following equation:

$$\Theta_i(t + \Delta t) = \langle \Theta_j \rangle_{|\mathbf{r}_i - \mathbf{r}_j| < R_n} + \eta_i,$$

where $\Theta_i(t)$ indicates the angle defining the direction of the velocity of particle i , while $\langle \Theta_j \rangle_{|\mathbf{r}_i - \mathbf{r}_j| < R_n}$ signifies the average angle of velocity vectors among the neighboring particles of particle i within a distance of R_n . Hence, the particle moves at constant speed v in new direction according to the following equation:

$$\mathbf{r}_i(t + \Delta t) = \mathbf{r}_i(t) + v\Delta t \begin{pmatrix} \cos \Theta_i(t) \\ \sin \Theta_i(t) \end{pmatrix},$$

where $\mathbf{r}_i(t)$ indicates the position of particle i at time t .

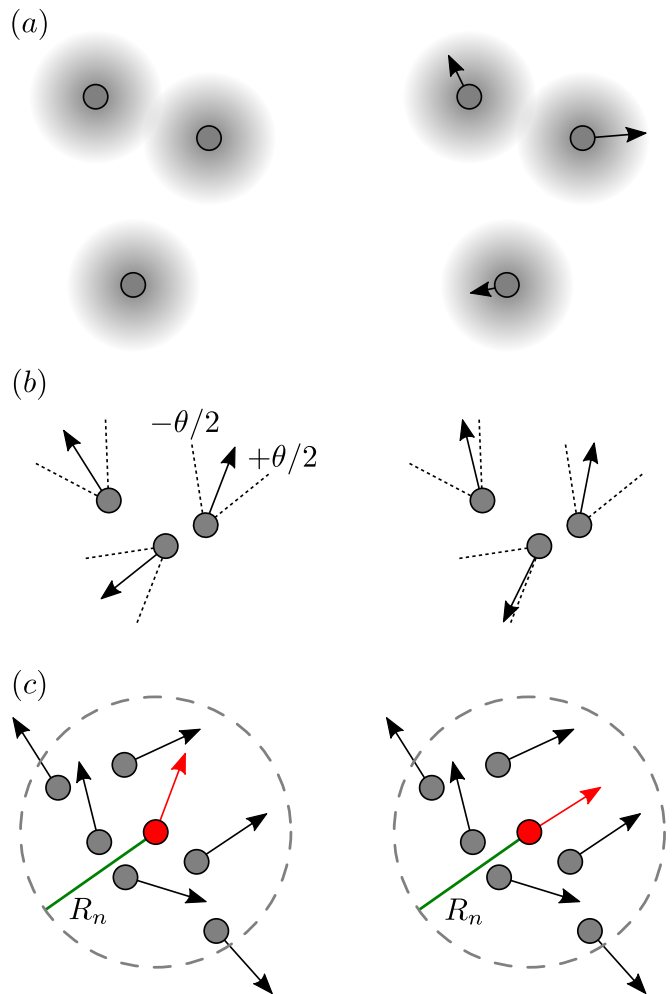


FIG. 1. **Schematic representation of the motion mechanisms for the three models.** (a) 2D Random Walk: at each time step, each particle selects a direction and a step length at random, following a uniform distribution for the angle and a half-gaussian for the step length. (b) Active Brownian Particle: at each time step, each particle updates its direction α by selecting uniformly at random a variation $\Delta\alpha$, with $\Delta\alpha$ constrained within the range $[-\frac{\theta}{2}, \frac{\theta}{2}]$, while maintaining of a constant velocity v . The smaller θ , the more the particle exhibits persistence of the direction of its motion. (c) Vicsek model: at each time step, particles align their direction with their neighbors by selecting the average direction over all neighbors within a given radius R_n . The alignment is altered by a noise η similar to the ABP model.

Contact network

Empirical data

A social interaction can mean many different behaviors, such as conversation, physical or eye contact, all of which hold significance in analyzing connections within a crowd. In our scenario we focus on a simpler interpretation, namely what we call a “contact”, which refers

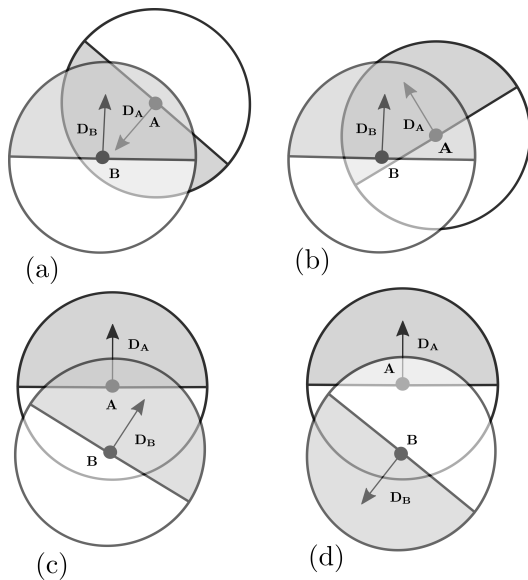


FIG. 2. **Typical four situations for particle contacts.** When two particles A and B are closer than the detection radius r_D , four different situations can occur depending on their respective orientation vectors D_A and D_B . As per our defined concept of contact, particles A and B are deemed to be in contact in configurations (a) and (b), as their are in both cases facing each other, *i.e.* in their respective front half-discs. In configurations (c) and (d) however, they are not in such a configuration and thus not considered to be in contact.

specifically to a physical closeness event. While physical proximity does not guarantee an interaction, past research indicates that it serves as a reliable indicator for an examination of the social context’s structure [43].

Such an approach was used by the SocioPatterns platform [6] for gathering empirical data about contacts between individuals. This platform has been extensively employed in the past decade to investigate interaction patterns in social settings [15, 24, 26, 33, 34, 48]. The system involves sensors affixed to participants’ nametags and antennas strategically positioned throughout the studied location to collect contact data from these sensors. Each sensor is equipped with an RFID chip which is able to detect other sensors within a proximity of approximately 1.5 meters. Notably, detection only occurs when two individuals are face-to-face, within each other’s front half-spheres, as the emitted signal is blocked by the human body. A contact event is defined by such proximity and geometry. These contacts are recorded at 20-second intervals and are capped at 40 simultaneous contacts for an individual within a 20-second time frame. According to the system design, contacts lasting at least 20 seconds are certain to be recorded, while shorter contacts may also be recorded with a probability that diminishes as their duration decreases.

While many different situations have been studied with this equipment, as a reference for the properties of empir-

ical contact networks we utilized data collected with the SocioPatterns platform during 4 face-to-face interactions conferences [14]. These data sets were preferred as they are characterised by an adult population, larger freedom of movement and less schedule constraints on the individuals’ behavior.

Particle models

In order to be able to compare empirical and artificial interactions, we detect contacts in the models in a way that mirrors the contact definition from the SocioPatterns data. An interaction between particles is thus defined by two factors: the closeness of particles to each other and the orientation with which particles can detect each other. As illustrated in Fig. 2, particles can only detect another particle present in their front half circle, which is characterized by a detection radius r_D and a detection vector named \vec{D}_i for particle with index i . For the sake of simplicity, we assume that the detection vector for each particle coincides with the velocity vector of the particle. This assumption is logically sound, as in most contact cases the orientation of the line of sight coincides with the movement. We further assume a similar detection radius of $r_D = 1$ for all particles.

Let us consider two particles A and B separated by a distance less than r_D . Let \vec{AB} be the vector from particle A to particle B. Particle B is then within the detection area of Particle A if $\vec{AB} \cdot \vec{D}_A \geq 0$. Similarly, Particle A is within the detection area of Particle B if $\vec{AB} \cdot \vec{D}_B \leq 0$. The fulfillment of both these conditions is necessary to establish that the two particles are in contact.

Contact networks comparison

To compare empirical and artificial contact networks, we focus on the distributions of three temporal properties of the contacts, namely contact duration, inter-contact duration and the number of contacts per pair of particles. In practice, for each pair of particles with indices i and j , we monitor their contact occurrences over time, generating a timeline of their interactions. The timeline of contacts between particle i and particle j takes the following form: $[t_1, t_2, t_3, t_4, \dots, t_k, \dots]$, where each odd-indexed element represents the beginning time of an interaction, and each even-indexed element represents the end time of the respective interaction. From this timeline array we can derive all the properties for a particular pair of particles, then join the results to obtain them for the whole population. For networks generated by the models, if the size of timeline array is an odd number (which indicates the contact was still ongoing at the end of the simulation), we simply drop the last element of the array.

RESULT

Temporal distributions form simple dynamics

Fig. 3 presents the contact duration, inter-contact duration, and number of contacts distributions for 2D Random Walk (2DRW), Active Brownian Particle (ABP) and Vicsek (VM) models respectively, for point particles and hard boundary conditions, and compares them with their empirical counterparts. In each model we tested several values for the parameter that fixes the level of noise (the diffusivity D for 2DRW, the angle range θ for ABP and VM).

Contact duration and number of contacts

Figure 3 (a) shows the distributions for the 2DRW for various diffusion coefficients: $D = 1, 0.1, 0.01, 0.001$. As expected, the distributions have an exponential shape, directly due to the uncorrelated randomness of the process. When D is large, particles easily escape the detection area of each other; consequently, they tend to stay in contact for shorter duration compared to when the diffusion coefficient is lower. This effect explains the relative positions of the distributions of contact duration. Similarly, distributions of number of contacts per pair of particles also exhibit an exponential tail and an ordering according to diffusivity. When two particles with a small diffusion coefficient break contact, they are less likely to move away quickly; as a result, they have a higher probability of making contact again in a shorter time period. Consequently, in this scenario, the number of contacts between two specific particles increases as the diffusivity decreases.

Figure 3 (b) shows the distributions for the ABP model. In this model, except for the case $\theta = 2\pi$ which is similar to the 2DRW, when particles come into contact with each other they tend to remain in contact for a longer duration, especially as θ decreases. This is mostly due to the fact that, when θ is small, particles in contact may have aligned directions, which are maintained for a while, leading to longer-lasting interactions. Contrarily, the ballistic aspect of their trajectories ensures that when particles break contact, they move away and stay apart longer, leading to a decrease in the total number of contacts as θ decreases.

Figure 3 (c) shows the distributions for the Vicsek model. This model is peculiar as it undergoes a phase transition as θ varies, from a disordered state for high values of θ to a flocking phase for low values of θ , with a critical value of approximately $\frac{\pi}{4}$ in our case (see SI). In the flocking phase, particles exhibit longer contact duration, as they move in groups, have aligned directions and thus stay close to each other. As θ increases, the alignment effect vanishes and the contact durations decrease.

In all cases though, the shape of the distribution remains exponential, similar to the 2DRW case. The behavior of the distribution of number of contacts is different, with a non-linearity directly due to the phase transition. While in the disordered phase the distribution is exponential, its shape changes towards higher values of n in the flocking phase, due to the numerous contacts which occur in the flocks.

As seen by comparing the previous results with Figure 3 (d), which shows the distributions for the four conferences, all of them are completely different from what is observed for empirical contacts. Empirical distributions exhibit a power law shape, which has been shown to be a characteristic commonly observed in human behavior. This discrepancy is not a surprise, as the models presented here incorporate dynamics that are far from being realistic. The shapes of the distributions are intricately tied to the specific dynamics inherent to each particle model, demonstrating the distinctive characteristics of each model and its interactions.

Inter-contact duration

However, we do observe something unexpected when examining the distributions of inter-contact duration. In all three models, this distribution exhibits the same power-law shape as it does in the data sets, and always with a similar exponent of -1.5 which is also observed for empirical contacts. For each model, this shape holds for all values of the parameter. The exponent is also the same in most cases, changing only slightly in the case of high diffusivity for 2DRW or long persistence for ABP. This remarkable fact seems to indicate that this particular property of contact dynamics between moving particles is largely independent from the details of the dynamics.

Focusing on the 2D random walk, arguments allow to relate the analytical derivation of this distribution to the distribution of first-passage times in a 1D random walk. Indeed, as they do not interact all particles have independent trajectories. The system can thus be reduced to a single pair of particles, for which we investigate the probability for two particles in contact to be in contact again after a time $\Delta\tau$. Classically, this 2D problem can be reduced to a 1D one by considering only the distance between the two particles. The evolution of this distance can be rewritten as a 1D random walk, which derivation gives a first passage time distribution with a power law tail of exponent -1.5 . However, this method is applicable only for particles moving on an infinite space. In our case, the hard boundaries make it more difficult to use a similar approach. Nonetheless, the fact that we do get the same exponent for the tail of the distribution seems to indicate that the effect of the boundaries probably does not change the core of the derivation.

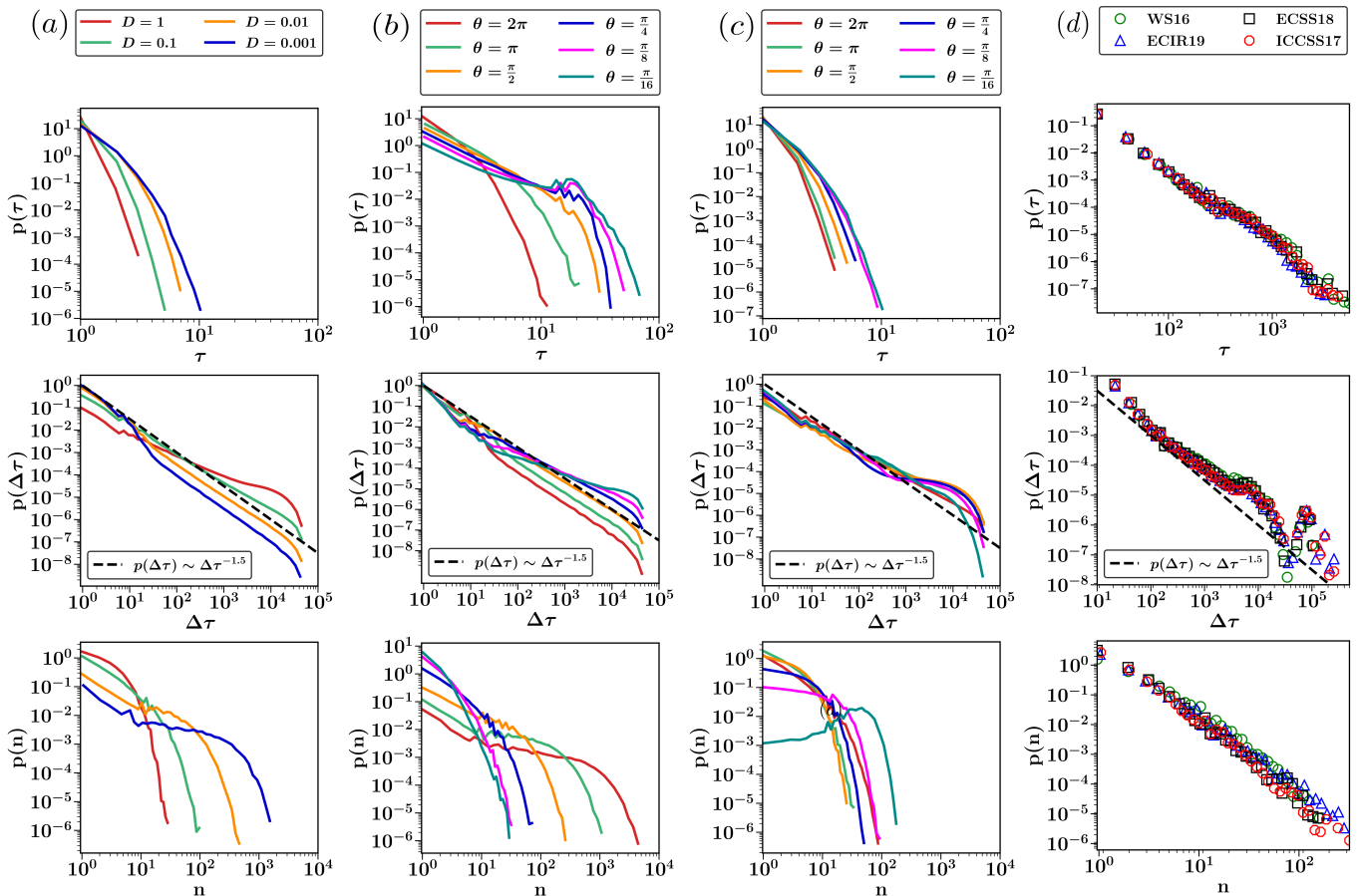


FIG. 3. **Comparison of the distributions of contact duration, inter-contact duration, and number of contacts for the different models.** (a) 2D Random Walk, (b) Active Brownian Particles, (c) Vicsek model, (d) conference data.

Furthermore, the fact that we get the same exponent in the other models lets us formulate a general hypothesis about the universality of this effect: if the motion of particles is “random enough” to be statistically equivalent to a random walk, then the distribution of inter-contact duration exhibits a power-law tail with exponent -1.5 .

Finally, the fact that we observe the same feature in empirical data of contacts between individuals lets us believe that the motion of human beings, although far from a random walk at the individual’s scale and at short time, is also sufficiently “random” to exhibit this property as well when considering a crowd over a certain time window.

Effect of particle size and boundary conditions on inter-contact durations

In order to better understand the possible mechanisms responsible for the peculiar shape of the distribution of inter-contact durations, we focus on the 2D Random Walk and modified the way particles interact as well as the boundary conditions. For the particle size, the main

difference between point particles and finite-size particles is the spatial organization: point particles can be as numerous as possible in a defined area of the simulated space and thus have unlimited simultaneous interactions, while the volume occupied by finite-size particles leads to a spatial organization and limits the number of simultaneous interactions. Changes in boundary conditions can modify the behaviour of a system. Hard boundaries impact the trajectories of particles while periodic boundaries do not; hard boundaries and periodic boundaries may impose finite-size effect on the global dynamics of the system while open boundaries do not.

As seen on Figure 4, changes in the particle size or in the boundary conditions do not affect at all the distribution of inter-contact durations, which retains in all cases its power law tail with an exponent -1.5 . In particular, it works for the case of point particles doing a random walk with no boundaries. This very simple setting allows us to analytically derive the distribution.

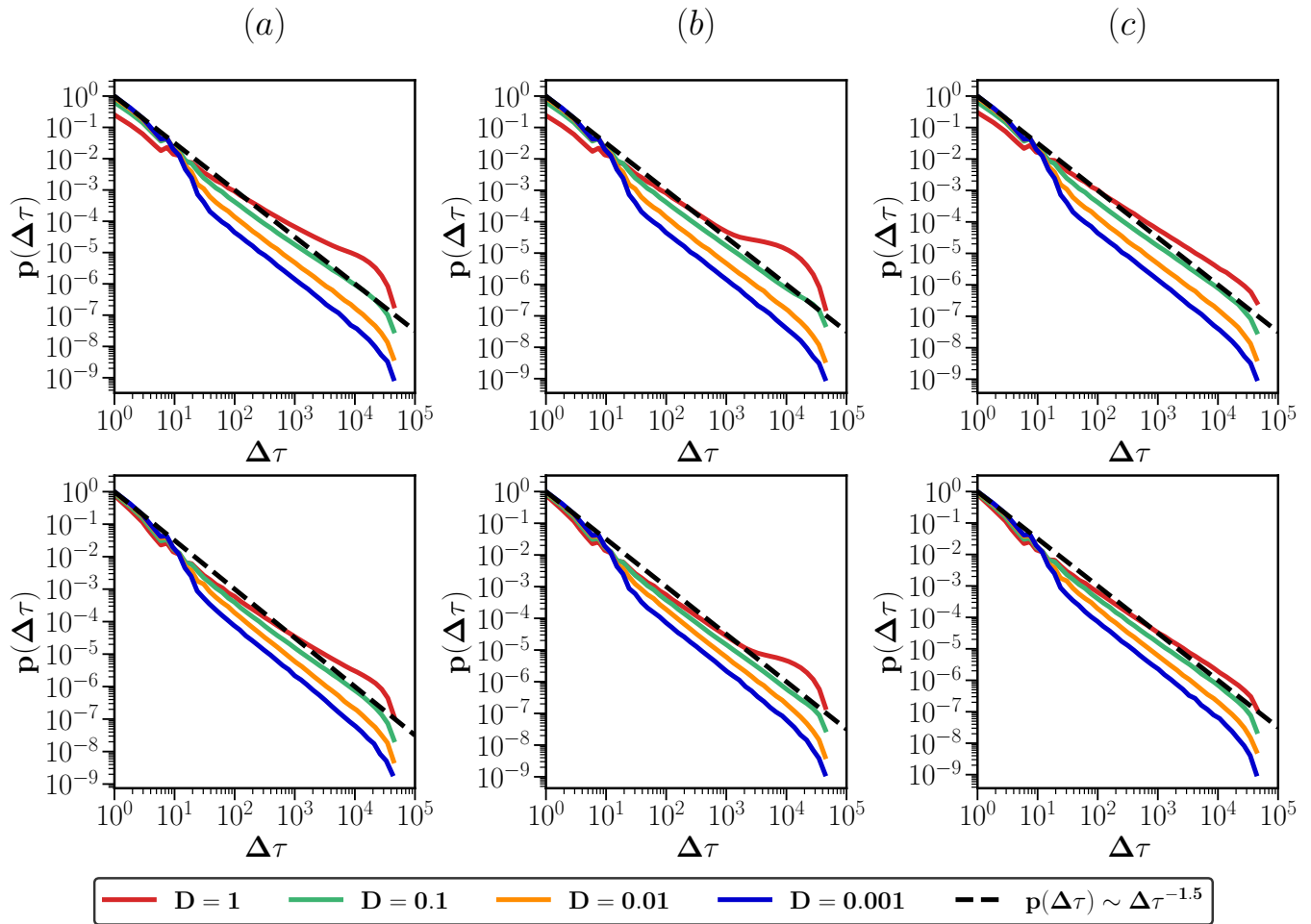


FIG. 4. Comparison of the distributions of inter-contact durations for the different version of the 2D Random Walk. Top: point particles, bottom: finite size particles. (a) Hard boundaries, (b) Periodic boundaries, (c) No boundaries.

Analytical argument

For the 2D Random Walk of point particles on an infinite space, we first acknowledge that the trajectories of particles are uncorrelated, as they do not interact. The distribution of inter-contact durations for a population of particles is thus strictly identical as the one for only 2 particles.

Then, the system can be reduced to tracking the evolution of the distance d between the two particles. If we define the random walk with the following process:

$$\mathbf{x}(t+1) = \mathbf{x}(t) + \mathbf{r} \quad (1)$$

with \mathbf{r} a random vector with an angle θ chosen uniformly in $[0, 2\pi[$ and a norm r chosen following the positive half of a gaussian, we have then:

$$\mathbf{d}_{12}(t+1) = \mathbf{d}_{12}(t) + \mathbf{s} \quad (2)$$

with $\mathbf{s} = \mathbf{r}_2 - \mathbf{r}_1$. Given Eq. (1), \mathbf{s} is also a random vector, which angle follows a uniform distribution. This

indicates that \mathbf{d} follows a 2D random walk process. As a consequence, the evolution of its norm d can be written as a 1D random walk process.

The distribution of inter-contact durations is then the distribution of the time it takes for d , starting from $d \leq r_D$, to become smaller than the detection radius r_D again. This distribution is exactly the distribution of first return times for the associated 1D random walk. Independently from the details of the stochastic process governing the evolution of d , this distribution has a power law tail $p(\Delta\tau) \sim \Delta\tau^{-3/2}$ [38], which is precisely the exponent we observe numerically.

CONCLUSION

In this study we focused on generating contact networks using three distinct two-dimensional particle dynamics models: 2D Random Walk, Active Brownian Particles, and Vicsek model. These contact networks serve as representations of pairwise interactions between parti-

cles in crowd models, offering insights into collective behavior and emergent properties of crowds. The primary objective was to compare the properties of empirical contact networks with those of networks generated by these models, and determine whether some of them could be explained by such simple mechanisms.

The analysis involved investigating the distributions of contact duration, inter-contact duration, and the number of contacts for the various particle models. We observed that the different models exhibited various characteristics related to their microscopic dynamics. However, the distribution of inter-contact duration exhibited in all cases a shape similar to what is found in empirical network of contacts, with a power-law tail of exponent -1.5 . Further simulations showed that this feature was retained even for a 2D random walk of point particles on a infinite space, which allowed us to relate it to a first-return time distribution in a 1D random walk, for which the classical results indeed gives a $-3/2$ exponent.

The presence of this tail in all variants of the 2D Random Walk indicates that this behaviour is not affected by either the fact that particles have a size, nor by the boundary conditions. Furthermore, the tail is retained in the other models too. This demonstrates that, while the dynamics of the particles might be very different, they are statistically equivalent to the 2D Random Walk with respect to the inter-contact durations. Finally, the presence of the same behaviour in empirical data seems to indicate that the trajectories of individuals, while far from being random, are nonetheless also statistically equivalent to random walks with respect to inter-contact durations.

In conclusion, this study provided insights into the dynamics of contact networks, shedding light on behavior in crowds. The findings contribute to the understanding of universal properties in pairwise interactions, even within the context of basic crowd models.

ACKNOWLEDGEMENT

R.M. is supported by an Emergence@INP grant from the CNRS. J.G. and M.G. are partially supported by the Agence Nationale de la Recherche (ANR) project DATAREDEX (ANR-19-CE46-0008).

AUTHOR CONTRIBUTIONS

M.G. proposed the core idea of the project. R.M., J.G. and M.G. contributed to the scientific discussions of the work. R.M. and J.G. wrote code and analyzed numerical and empirical data. R.M., J.G. and M.G. wrote and reviewed the final manuscript.

COMPETING INTEREST

The authors declare no competing interests.

* mathieu.genois@cpt.univ-mrs.fr

- [1] Paolo Bajardi, Alain Barrat, Fabrizio Natale, Lara Savini, and Vittoria Colizza. Dynamical patterns of cattle trade movements. *PLoS one*, 6(5):e19869, 2011.
- [2] Alain Barrat, Ciro Cattuto, Vittoria Colizza, Francesco Gesualdo, Lorenzo Isella, Elisabetta Pandolfi, J F Pinton, Lucilla Ravà, Caterina Rizzo, Mariateresa Romano, et al. Empirical temporal networks of face-to-face human interactions. *The European Physical Journal Special Topics*, 222:1295–1309, 2013.
- [3] Danielle S Bassett, Nicholas F Wymbs, M Puck Rombach, Mason A Porter, Peter J Mucha, and Scott T Grafton. Task-based core-periphery organization of human brain dynamics. *PLoS computational biology*, 9(9):e1003171, 2013.
- [4] Danielle S Bassett, Muzhi Yang, Nicholas F Wymbs, and Scott T Grafton. Learning-induced autonomy of sensorimotor systems. *Nature neuroscience*, 18(5):744–751, 2015.
- [5] Benjamin Blonder and Anna Dornhaus. Time-ordered networks reveal limitations to information flow in ant colonies. *PLoS one*, 6(5):e20298, 2011.
- [6] Ciro Cattuto, Wouter Van den Broeck, Alain Barrat, Vittoria Colizza, Jean-François Pinton, and Alessandro Vespignani. Dynamics of person-to-person interactions from distributed rfid sensor networks. *PLoS one*, 5(7):e11596, 2010.
- [7] Yoon-Sik Cho, Aram Galstyan, P Jeffrey Brantingham, and George Tita. Latent self-exciting point process model for spatial-temporal networks. *arXiv preprint arXiv:1302.2671*, 2013.
- [8] Margaret C Crofoot, Daniel I Rubenstein, Arun S Maiya, and Tanya Y Berger-Wolf. Aggression, grooming and group-level cooperation in white-faced capuchins (*cebus capucinus*): Insights from social networks. *American Journal of Primatology*, 73(8):821–833, 2011.
- [9] Darren P Croft, Jens Krause, and Richard James. Social networks in the guppy (*poecilia reticulata*). *Proceedings of the Royal Society of London. Series B: Biological Sciences*, 271(suppl.6):S516–S519, 2004.
- [10] Nathan Eagle and Alex Pentland. Reality mining: sensing complex social systems. *Personal and ubiquitous computing*, 10:255–268, 2006.
- [11] Holger Ebel, Lutz-Ingo Mielsch, and Stefan Bornholdt. Scale-free topology of e-mail networks. *Physical review E*, 66(3):035103, 2002.
- [12] Jean-Pierre Eckmann, Elisha Moses, and Danilo Sergi. Entropy of dialogues creates coherent structures in e-mail traffic. *Proceedings of the National Academy of Sciences*, 101(40):14333–14337, 2004.
- [13] Francesco Ficarola and Andrea Vitaletti. Capturing interactions in face-to-face social networks. In *WEBIST*, pages 613–620, 2015.
- [14] Gauvin, Laetitia and Géniois, Mathieu and Karsai, Márton and Kivelä, Mikko and Takaguchi, Taro and Valdano, Eugenio and Vestergaard, Christian L. Ran-

- domized reference models for temporal networks. *SIAM Review*, 64(4):763–830, 2022.
- [15] Mathieu Génois and Alain Barrat. Can co-location be used as a proxy for face-to-face contacts? *EPJ Data Science*, 7(1):1–18, 2018.
- [16] Petter Holme. Network reachability of real-world contact sequences. *Physical Review E*, 71(4):046119, 2005.
- [17] Petter Holme. Epidemiologically optimal static networks from temporal network data. *PLoS computational biology*, 9(7):e1003142, 2013.
- [18] Petter Holme. Analyzing temporal networks in social media. *Proceedings of the IEEE*, 102(12):1922–1933, 2014.
- [19] Petter Holme and Jari Saramäki. Temporal networks. *Physics reports*, 519(3):97–125, 2012.
- [20] Lorenzo Isella, Mariateresa Romano, Alain Barrat, Ciro Cattuto, Vittoria Colizza, Wouter Van den Broeck, Francesco Gesualdo, Elisabetta Pandolfi, Lucilla Ravà, Caterina Rizzo, et al. Close encounters in a pediatric ward: measuring face-to-face proximity and mixing patterns with wearable sensors. *PloS one*, 6(2):e17144, 2011.
- [21] Zhi-Qiang Jiang, Wen-Jie Xie, Ming-Xia Li, Boris Podobnik, Wei-Xing Zhou, and H Eugene Stanley. Calling patterns in human communication dynamics. *Proceedings of the National Academy of Sciences*, 110(5):1600–1605, 2013.
- [22] Márton Karsai, Mikko Kivela, Raj Kumar Pan, Kimmo Kaski, János Kertész, A-L Barabási, and Jari Saramäki. Small but slow world: How network topology and burstiness slow down spreading. *Physical Review E*, 83(2):025102, 2011.
- [23] Mark Kibanov, Martin Atzmueller, Christoph Scholz, and Gerd Stumme. Temporal evolution of contacts and communities in networks of face-to-face human interactions. *Science China Information Sciences*, 57:1–17, 2014.
- [24] Moses C Kiti, Michele Tizzoni, Timothy M Kinyanjui, Dorothy C Koech, Patrick K Munywoki, Milosch Meriac, Luca Cappa, André Panisson, Alain Barrat, Ciro Cattuto, et al. Quantifying social contacts in a household setting of rural kenya using wearable proximity sensors. *EPJ data science*, 5:1–21, 2016.
- [25] Mikko Kivela, Raj Kumar Pan, Kimmo Kaski, János Kertész, Jari Saramäki, and Márton Karsai. Multi-scale analysis of spreading in a large communication network. *Journal of Statistical Mechanics: Theory and Experiment*, 2012(03):P03005, 2012.
- [26] Inkeri Kontro and Mathieu Génois. Combining surveys and sensors to explore student behaviour. *Education Sciences*, 10(3):68, 2020.
- [27] Gregory F Lawler and Vlada Limic. *Random walk: a modern introduction*, volume 123. Cambridge University Press, 2010.
- [28] Didier Le Bail, Mathieu Génois, and Alain Barrat. Modeling framework unifying contact and social networks. *Phys. Rev. E*, 107:024301, Feb 2023.
- [29] Sungmin Lee, Luis EC Rocha, Fredrik Liljeros, and Petter Holme. Exploiting temporal network structures of human interaction to effectively immunize populations. *PloS one*, 7(5):e36439, 2012.
- [30] Alexander V Mantzaris, Danielle S Bassett, Nicholas F Wymbs, Ernesto Estrada, Mason A Porter, Peter J Mucha, Scott T Grafton, and Desmond J Higham. Dynamic network centrality summarizes learning in the human brain. *Journal of Complex Networks*, 1(1):83–92, 2013.
- [31] Naoki Masuda, Taro Takaguchi, Nobuo Sato, and Kazuo Yano. Self-exciting point process modeling of conversation event sequences. *Temporal networks*, pages 245–264, 2013.
- [32] James Moody, Daniel McFarland, and Skye BenderdeMoll. Dynamic network visualization. *American journal of sociology*, 110(4):1206–1241, 2005.
- [33] Marcos Oliveira, Fariba Karimi, Maria Zens, Johann Schaible, Mathieu Génois, and Markus Strohmaier. Group mixing drives inequality in face-to-face gatherings. *Communications Physics*, 5(1):127, 2022.
- [34] Laura Ozella, Daniela Paolotti, Guilherme Lichand, Jorge P Rodríguez, Simon Haenni, John Phuka, Onicio B Leal-Neto, and Ciro Cattuto. Using wearable proximity sensors to characterize social contact patterns in a village of rural malawi. *EPJ Data Science*, 10(1):46, 2021.
- [35] Raj Kumar Pan and Jari Saramäki. Path lengths, correlations, and centrality in temporal networks. *Physical Review E*, 84(1):016105, 2011.
- [36] André Panisson, Laetitia Gauvin, Alain Barrat, and Ciro Cattuto. Fingerprinting temporal networks of close-range human proximity. In *2013 IEEE international conference on pervasive computing and communications workshops (PERCOM workshops)*, pages 261–266. IEEE, 2013.
- [37] N. Perra, B. Gonçalves, R. Pastor-Satorras, and A. Vespignani. Activity driven modeling of time varying networks. *Scientific Reports*, 2(1), jun 2012.
- [38] Sidney Redner. *A Guide to First-Passage Processes*. Cambridge University Press, 2001.
- [39] Luis EC Rocha and Vincent D Blondel. Bursts of vertex activation and epidemics in evolving networks. *PLoS computational biology*, 9(3):e1002974, 2013.
- [40] Pawel Romanczuk, Markus Bär, Werner Ebeling, Benjamin Lindner, and Lutz Schimansky-Geier. Active brownian particles: From individual to collective stochastic dynamics. *The European Physical Journal Special Topics*, 202:1–162, 2012.
- [41] Martin Rosvall and Carl T Bergstrom. Mapping change in large networks. *PloS one*, 5(1):e8694, 2010.
- [42] Martin Rosvall, Alcides V Esquivel, Andrea Lancichinetti, Jevin D West, and Renaud Lambiotte. Memory in network flows and its effects on spreading dynamics and community detection. *Nature communications*, 5(1):4630, 2014.
- [43] Johann Schaible, Marcos Oliveira, Maria Zens, and Mathieu Génois. Sensing close-range proximity for studying face-to-face interaction. In *Handbook of Computational Social Science, Volume 1*, pages 219–239. Routledge, 2021.
- [44] Michele Starnini, Andrea Baronchelli, and Romualdo Pastor-Satorras. Modeling human dynamics of face-to-face interaction networks. *Physical review letters*, 110(16):168701, 2013.
- [45] Juliette Stehlé, Nicolas Voirin, Alain Barrat, Ciro Cattuto, Vittoria Colizza, Lorenzo Isella, Corinne Régis, Jean-François Pinton, Naghm Khanafer, Wouter Van den Broeck, et al. Simulation of an seir infectious disease model on the dynamic contact network of conference attendees. *BMC medicine*, 9(1):1–15, 2011.
- [46] Siva R Sundaresan, Ilya R Fischhoff, Jonathan Dushoff, and Daniel I Rubenstein. Network metrics reveal differences in social organization between two fission–fusion species, grevy’s zebra and onager. *Oecologia*, 151:140–149, 2007.

- [47] Chayant Tantipathananandh, Tanya Berger-Wolf, and David Kempe. A framework for community identification in dynamic social networks. In Proceedings of the 13th ACM SIGKDD international conference on Knowledge discovery and data mining, pages 717–726, 2007.
- [48] Philippe Vanhems, Alain Barrat, Ciro Cattuto, Jean-François Pinton, Nagham Khanafer, Corinne Régis, Byeul-a Kim, Brigitte Comte, and Nicolas Voirin. Estimating potential infection transmission routes in hospital wards using wearable proximity sensors. PloS one, 8(9):e73970, 2013.
- [49] Christian L Vestergaard, Mathieu Génois, and Alain Barrat. How memory generates heterogeneous dynamics in temporal networks. Physical Review E, 90(4):042805, 2014.
- [50] Nicolas Voirin, Cécile Payet, Alain Barrat, Ciro Cattuto, Nagham Khanafer, Corinne Régis, Byeul-a Kim, Brigitte Comte, Jean-Sébastien Casalegno, Bruno Lina, et al. Combining high-resolution contact data with virological data to investigate influenza transmission in a tertiary care hospital. Infection Control & Hospital Epidemiology, 36(3):254–260, 2015.
- [51] Erik Volz and Lauren Ancel Meyers. Susceptible–infected–recovered epidemics in dynamic contact networks. Proceedings of the Royal Society B: Biological Sciences, 274(1628):2925–2934, 2007.